A new RISE-based adaptive control of PKMs: design, stability analysis and experiments

Moussab Bennehar, Ahmed Chemori, Mohamed Bouri, Laurent Frédéric Jenni, François Pierrot

To appear in the *International Journal of Control*
Vol. 00, No. 00, Month 20XX, 1–18

A new RISE-based adaptive control of PKMs: design, stability analysis and experiments

GUIDE

Adaptive RISE-based Control of PKMs: Application to the Delta robot

M. Bennehar[a*], A. Chemori[a], M. Bouri[b], L.F. Jenni[b] and F. Pierrot[a]

[a]*LIRMM, Univ. Montpellier-CNRS, 161 rue Ada, 34090 Montpellier, France;* [b]*LSRO-EPFL, Station 9, Lausanne CH-1015, Switzerland*

(*v5.0 released February 2015*)

This paper deals with a new adaptive controller for parallel kinematic manipulators (PKMs) based on the recently developed Robust Integral of the Sign of the Error (RISE) control strategy. The original RISE controller is based only on feedback information and does not take advantage of the dynamics of the system. Consequently, the performance of the closed-loop system may be poor compared to more advanced model-based control strategies. We propose in this work to enhance RISE control by including some knowledge about the dynamics of the robot to improve its tracking performance. More precisely, we augment original RISE with a model-based adaptive feedforward term that compensates for the inherent nonlinearities in the closed-loop system. To demonstrate the relevance of the proposed contribution, real-time experiments are conducted on the Delta robot; a three degree-of-freedom (3-DOF) PKM.

Keywords: Adaptive control; parallel manipulators; RISE; Delta robot.

1. Introduction

The popularity of Parallel Kinematic Manipulators (PKMs) has tremendously grown since Prof. Raymond Clavel invented the first Delta robot in the early 80s Clavel (1985). His idea of using lightweight parallelograms and base-mounted actuators has led to the development of extremely fast PKMs capable of reaching up to 100 G of experimental platform acceleration. For this reason, the first industrial Delta-like PKMs mainly targeted high speed pick-and-place applications in packaging industry Nabat, de la O Rodriguez, Company, Krut, and Pierrot (2005). Several years later, PKMs started gaining an increasing interest in diverse fields such as food packaging Connolly (2007), electronics Dachang, Yanping, and Yuefa (2005), machining Shayya, Krut, Company, Baradat, and Pierrot (2014b) and even surgical interventions Deblaise and Maurine (2005). Indeed, in addition to being extremely fast, PKMs are well known for their accuracy, stiffness and high load/weight ratio Merlet (2006), among other impressive qualities. To satisfy industrial needs in terms of dexterity and workspace size, researchers focus mostly on the design synthesis and optimization of the mechanical structure of the PKM Shayya, Krut, Company, Baradat, and Pierrot (2014a). This research trend seeks to increase the acceptance of PKMs and adapt them to be used in various industrial tasks Patel and George (2012). Indeed, several studies has culminated in the development of stiffer and less cumbersome PKMs having a larger workspace and relatively simpler modeling Company, Pierrot, Krut, Baradat, and Nabat (2011); Germain, Caro, Briot, and Wenger (2013). Nevertheless, to achieve the required tracking accuracy, the use of sophisticated modern control strategies is unavoidable He, Jiang, Cong, and Ye (2007). Especially on high accelerations where the control problem becomes a very challenging task due to the important nonlinearities and the numerous undesired phenomena associated with it Sartori Natal, Chemori, Pierrot, and

*Corresponding author. Email: bennehar@lirmm.fr

Company (2010).

The earlier control schemes that have been applied on PKMs were the classical single axis PID controllers Ziegler and Nichols (1942). These controllers are still the most used in industrial manipulators thanks to their simplicity, efficiency, clearer physical meanings and intuitive tuning Kiam, Chong, and Yun (2005). However, PID controllers are not well suited for nonlinear systems such as mechanical manipulators and may lead to very poor performance, especially on high accelerations, and may even cause instability Sartori Natal, Chemori, and Pierrot (2015). In order to improve the performance of any mechanical manipulator, the inherent nonlinearities have to be accounted for by considering the use of the dynamic model in the control loop Siciliano, Sciavicco, Villani, and Oriolo (2009). The simplest developed controller that takes advantages of such strategy is the PD with gravity compensation controller Chifu, Qitao, Hongzhou, O. Ogbobe, and Junwei (2010). In this controller an additional control term based on the configuration of the manipulator is added to the PD feedback loop in order to compensate for the gravity effects. The same strategy is adopted for more complex mode-based controllers in a way that a nonlinear loop based on the dynamics of the manipulator is added to the PD controller in order to compensate for the inherent nonlinearities. Examples of such controllers are the PD with computed feedforward Sartori Natal, Chemori, Michelin, and Pierrot (2012), Augmented PD (APD) Zhang, Cong, Shang, Li, and Jiang (2007) and the Computed Torque (CT) Asgari and Ardestani (2015) controllers. Nevertheless, to properly compensate for such nonlinearities, the dynamic model of the manipulator has to be precisely known, whereas this is impossible in practice. Indeed, the dynamic parameters of the manipulator do not accurately match the values of its CAD design due to manufacturing assembly defects. Furthermore, the dynamic model can be time-varying due to operational conditions (e. g. payload change).

To cope with the uncertainties issue in non-adaptive controllers, model-based Adaptive Control (AC) has been applied to mechanical manipulators Craig, Hsu, and Sastry (1987). In this class of controllers, an additional loop is added to the controller whose job is to online estimate the uncertain and/or unknown parameters used by the model-based block in the control scheme. However, despite its relevance, model-based AC did not gain the same interest as in serial manipulators. In fact, very few papers addressed AC of PKMs. For instance, in Honegger, Codourey, and Burdet (1997), the Desired Compensation Adaption Law (DCAL) Sadegh and Horowitz (1990) has been applied on a 6-DOF PKM. In this work, the control law consisted of a PD control with an adaptive feedforward term based on the dynamics of the manipulator and the desired trajectories. The dynamic parameters of the robot were supposed unknown and their adaptation was adjusted according to the gradient decent algorithm that minimizes the joint tracking errors. In a more recent work Shang and Cong (2010), a task-space AC for PKMs is developed. The gradient decent method is applied to derive the parameters adaptation law that minimize the Cartesian tracking errors. Real-time experiments on a 2-DOFs Redundantly Actuated (RA-PKM) demonstrated that the proposed adaptive controller outperforms its non-adaptive counterpart. The same authors of the previous work proposed in Shang, Cong, and Ge (2012) an adaptive version of the task-space CT controller based on Craig et al. (1987). Experimental comparative study which were conducted on a 2-DOF RA-PKM demonstrated that the adaptive scheme significantly reduced the tracking errors compared to the non-adaptive scheme. Nevertheless, adaptive controllers show two major drawbacks that limit their expansion in real-time applications. First, most of the developed adaptive schemes consider only the nonlinearities related to the dynamic characteristics of the manipulator. Whereas in practice, the system is subject to different types of disturbances such as external disturbances and unmodeled phenomena. Second, during the transient phase, the system is highly nonlinear since the nonlinearities are not yet correctly compensated. Therefore, those nonlinearities will be accommodated by the single axis PD feedback part of the control scheme, which is not suitable for dealing with such disturbances.

Recently, a new robust feedback control strategy for nonlinear systems was developed in Xian, Dawson, de Queiroz, and Chen (2004) called the Robust Integral of the Sign of the Error (RISE).

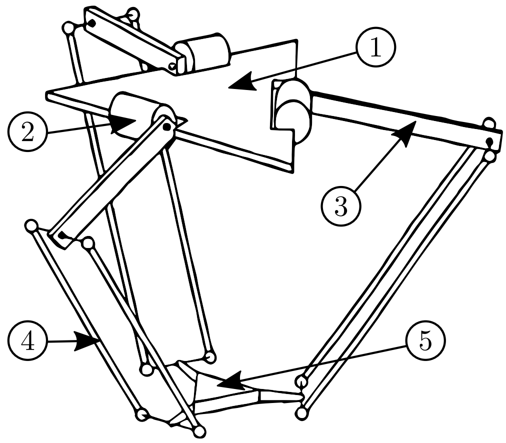

Figure 1. Schematic view of Delta PKM: (1) fixed base, (2) actuator, (3) rear-arm, (4) forearm, (5) traveling plate.

This control strategy can accommodate a large class of different uncertainties and disturbances provided some non-restrictive continuity and boundedness assumptions. The RISE control strategy has been widely endorsed since its first appearance. It has been successfully applied on various nonlinear systems such as hard drives Taktak-Meziou, Chemori, Ghommam, and Derbel (2015), DC motors Patre, MacKunis, Makkar, and Dixon (2008), underwater vehicles Fischer, Hughes, Walters, Schwartz, and Dixon (2014), etc. It has been reported in Patre et al. (2008) that the RISE controller can be augmented with an additional model-based control term in order to improve the overall performance of the system.

In this work we propose to augment the RISE controller with a model-based adaptive feedforward term to improve the tracking performance of the closed-loop system. This work can be considered as an extension of Bennehar, Chemori, and Pierrot (2014) where a RISE-based adaptive controller was applied on a 3-DOF redundantly actuated PKM. The main contribution of this work compared to Bennehar et al. (2014) is the stability analysis of the closed-loop system. To demonstrate the superiority of the proposed controller, we experimentally validate both, the original and adaptive, RISE controllers on a 3-DOF Delta PKM. This paper is organized as follows; in section 2, the dynamic modelling of the Delta robot is recalled. In section 3, some properties of the dynamics, required for the theoretical development, are enumerated. Section 4, the original RISE controller is presented. Section 5 is devoted to the development of the proposed adaptive controller. In section 6, the stability of the closed-loop system is analyzed. Section 7 is dedicated to the real-time experiments and results obtained on the Delta robot. A general conclusion of the current work is provided in 8.

2. Dynamic Modeling of DELTA PKM

The Delta robot is a 3-DOF PKM developed by Prof. Reymond Clavel at EPFL. It is composed of three parallel kinematic chains linked at the traveling plate. Each chain is a serial arrangement of a revolute actuator, a rear-arm and a forearm (composed of two parallel rods forming a parallelogram). The rear-arms and the forearms are linked through ball-and-socket passive joints. The parallelograms structure of the forearms ensure that the traveling plate stays always parallel to the fixed base. Figure 1 shows a schematic design of a typical Delta robot. The main geometric and dynamic parameters of the Delta robot used for experiments in this paper are summarized in Table 1.

For model-based control, an efficient dynamic model that predicts the behavior of the system is required. This dynamic model in model-based controllers is included in the control loop in order to

Table 1. Main parameters of the Delta robot.

Parameter	Value
Rear-arm's length	240 mm
Rear-arm's mass	0.22 kg
Forearm's length	480 mm
Forearm's mass	0.084 kg
Actuator's inertia	$1.82 \,.\, 10^{-3}$ kg.m^2
Traveling-plate's mass	0.305 kg

enhance the overall performance of the closed-loop system. For the dynamic modeling of the Delta-3 parallel robot, the following simplifying assumptions, which are common to Delta-like PKMs, are considered:

Assumption 1: *The rotational inertia of the forearms is neglected.*

Assumption 2: *The mass of each forearm m_{fa} is split up into two point-masses located at the forearm both ends.*

Assumption 3: *Friction in all passive and active joints is neglected.*

These assumptions allow for a significant simplification of the dynamic model of the Delta PKM without important loss of accuracy. Indeed, the complexity of the dynamic model mainly comes from the movements of the forearms. Neglecting their rotational inertia enables to consider that the linking force between the traveling plate and the arms is oriented towards the forearms direction Codourey (1998).

In order to simplify the establishment of the dynamic model of the Delta robot, let us introduce its Jacobian matrix $J \in \mathbb{R}^{3\times3}$. The Jacobian matrix expresses the relationship between the Cartesian velocities of the traveling plate $\dot{X} \in \mathbb{R}^3$ and the joint velocities $\dot{q} \in \mathbb{R}^3$ as follows:

$$\dot{X} = J\dot{q}. \tag{1}$$

It is worth mentioning that the Jacobian matrix is usually obtained by differentiating the loop closure constraints Codourey (1998).

Given the previously mentioned simplifying hypotheses, the dynamics of the Delta robot can be reduced to analyzing the dynamics of four bodies; namely, the traveling plate and the three rear-arms.

Regarding the traveling plate dynamics, two different forces acting on it can be distinguished:

- The gravity force $F_{p_G} \triangleq m_p G$, where m_p is the mass of the traveling plate including the point-masses of the forearms and eventual payload. The gravity vector $G \in \mathbb{R}^3$ is given by:

  $$G \triangleq [0 \; 0 \; -g],$$

  where $g = 9.8$ m/s^2 is the gravity constant.
- The inertial force $F_{p_a} \in \mathbb{R}^3$ due to the acceleration of the traveling plate given by:

  $$F_{p_a} \triangleq m_p \ddot{X},$$

  where $\ddot{X} \in \mathbb{R}^3$ denotes the traveling plate's acceleration vector.

The contribution of these two forces to the actuators, denoted by τ_p, can be computed by means of the Jacobian matrix as follows

$$\tau_p = J^T m_p \left(G + \ddot{X}\right). \tag{2}$$

Regarding the rear-arms, three torques are acting on them:

- The actuator torque $\tau \in \mathbb{R}^3$.
- The torque due to the acceleration of the arms given by:

$$\tau_{r_a} = I_r \ddot{q},$$

where $I_r \in \mathbb{R}^{3\times3}$ is a diagonal matrix gathering the inertia of the actuators, the forearms and the point-masses and $\ddot{q} \in \mathbb{R}^3$ denotes the joint accelerations.
- The torque produced by the gravitational force given by:

$$\tau_{r_G} = m_r r_G cos(q),$$

where m_r is the mass of one rear-arm in addition to the corresponding half-mass, r_G is the center of mass of the rear-arm and $cos(q) \triangleq [cos(q_1)\ cos(q_2)\ \ cos(q_3)]$, being $q_i, i = 1 \dots 3$ the angular position of the ith joint.

Applying the virtual work principle, which states that the sum of all non-inertial forces must be equal to the sum of all inertial ones, we obtain:

$$\tau + J^T m_p G + m_r r_G cos(q) = I_r \ddot{q} + J^T m_p \ddot{X}. \tag{3}$$

Given the fact that the Cartesian and joint accelerations are linked through the following kinematic relationships:

$$\ddot{X} = J\ddot{q} + \dot{J}\dot{q}, \tag{4}$$

where $\dot{J}$ is the time derivative of J, and after rearranging the terms, the inverse dynamic model of the delta robot can be put into the standard joint space form as follows:

$$M(q)\ddot{q} + C(q, \dot{q})\dot{q} + G(q) = \tau, \tag{5}$$

where

- $M(q) = I_r + m_p J^T J$ is the mass matrix of the robot,
- $C(q, \dot{q}) = m_p J^T \dot{J}$ is its Coriolis and centrifugal forces matrix and
- $G(q) = -J^T m_p G - m_r r_G cos(q)$

3. Reformulation and Properties of Delta PKM's Dynamics

Model-based adaptive controllers rely mainly on a fundamental property of the manipulator's dynamics. This property consists in the linearity of the dynamics with respect to the dynamic parameters characterizing the manipulator mechanical structure such as inertia and masses Craig et al. (1987); Siciliano et al. (2009). Hence, the inverse dynamics could be rewritten in a linear form with respect to a chosen vector of parameters.

Consider the general form of the inverse dynamics of a n-DOF PKM given by (5). The linear in the parameters reformulation of the dynamics can be expressed as:

$$M(q)\ddot{q} + C(q, \dot{q})\dot{q} + G(q) = Y(q, \dot{q}, \ddot{q})\theta, \tag{6}$$

where $Y(.) \in \mathbb{R}^{n\times p}$ is called the regression matrix, which is a nonlinear function of the joint positions $q \in \mathbb{R}^3$, velocities $\dot{q}$ and accelerations $\ddot{q}$, and $\theta \in \mathbb{R}^p$ is the vector of the parameters of the robot to be estimated.

It is worth noting that not all the dynamic parameters of the manipulators should be considered unknown/uncertain. Indeed, we may have a good knowledge about some parameters while other ones can be unknown, uncertain or time-varying. In this case, the set of parameters can be divided into two sets, namely, known and unknown parameters. A typical example is when considering the variations of the dynamic parameters of the robot's traveling plate due to payload handling. In such situation, it would be interesting to consider only the mass and inertia of the traveling plate to be estimated. In this case, the reformulation of the dynamics can be rewritten as follows Ortega and Spong (1989):

$$M(q)\ddot{q} + C(q, \dot{q})\dot{q} + G(q) = Y_n(q, \dot{q}, \ddot{q})\theta_n + Y_u(q, \dot{q}, \ddot{q})\theta_u, \tag{7}$$

where $\theta_n \in \mathbb{R}^{p_n}$ contains known parameters and $\theta_u \in \mathbb{R}^{p_u}$ contains only those parameters needed to to be estimated Ortega and Spong (1989). $Y_n(q, \dot{q}, \ddot{q}) \in \mathbb{R}^{n \times p_n}$ and $Y_u(q, \dot{q}, \ddot{q}) \in \mathbb{R}^{n \times p_u}$ are partial regression matrices.

Moreover, the following properties, common to all mechanical manipulators, are considered:

Property 1: The mass matrix $M(q)$ is symmetric, positive-definite and satisfies the following inequality $\forall y \in \mathbb{R}^n$:

$$\underline{M} \left\| y \right\|^2 \leq y^T M(q) y \leq \bar{M}(q) \left\| y \right\|^2 \tag{8}$$

for some known positive constant $\underline{M}$ and some positive nondecreasing function $\bar{M}(q)$.

Property 2: If $q(t), \dot{q}(t)$ are bounded, then the elements of $M(q)$, $C(q, \dot{q})$ and $G(q)$ are second-order differentiable with respect to $q(t)$ and $\dot{q}(t)$, respectively.

4. Background on RISE Control

RISE is a recently developed robust feedback control strategy for uncertain nonlinear systems Xian et al. (2004). The main advantage of RISE is that, based on limited assumptions about the system, it is able to compensate for a large class of uncertainties. This is of a tremendous importance for mechanical manipulator since they are known for the abundance of uncertainties in their dynamics and the environment. Examples of such uncertainties include non-modeled phenomena, payload variations, uncertain dynamic properties, etc. Therefore, for an efficient tracking of the desired trajectories, all of the uncertainties have to be considered in the control loop. RISE accommodates for a general class of uncertainties thanks to its unique structure as it will be explained in the sequel.

Let the desired joint positions, velocities and accelerations be denoted by $q_d(t), \dot{q}_d(t)$ and $\ddot{q}(t)$, respectively. Now, consider the combined velocity-position tracking error expressed as:

$$r(t) = \dot{e}(t) + \alpha_1 e(t), \tag{9}$$

where $e(t) \triangleq q_d(t) - q(t)$ is the joint position tracking error and α_1 is a positive control design gain. To simplify the subsequent mathematical developments, define the following auxiliary error signal

$$\nu(t) = \dot{r}(t) + \alpha_2 r(t) \tag{10}$$

where α_2 is positive control design parameter. The open-loop error system can be obtained by multiplying (10) by $M(q)$ and using (5) and (9) yielding

$$M(q)r = C(q,\dot{q})\dot{q} + G(q) + M(q)\left(\ddot{q}_d + \alpha_1\dot{e} + \alpha_2 r\right) - \tau(t) \tag{11}$$

where $\ddot{q}_d$ denotes the desired acceleration trajectory. As explained in Xian et al. (2004), based on (11), the RISE feedback control law is given by

$$\tau_{RISE}(t) = (k_s+1)\,r(t) - (k_s+1)\,r(t_0) + \int_{t_0}^{t}\left[(k_s+1)\,\alpha_2 r(\tau) + \beta\,\mathrm{sgn}\left(r\left(\tau\right)\right)\right]d\tau \tag{12}$$

where k_s is a positive control design gain. Substituting the control law in (12) to the open-loop error dynamics in (11) and taking the first time derivative, we obtain

$$M(q)\dot{\nu} = -\frac{1}{2}\dot{M}(q)\nu + N(.) - \dot{\tau}_{RISE} - r \tag{13}$$

where $N(.)$ denotes a nonlinear unmeasurable auxiliary function expressed as

$$\begin{aligned} N(.) = {} & \dot{M}(q)\left(\alpha_1\left(r - \alpha_1 e\right) + \alpha_2 r\right) + M(q)\left(\alpha_1\left(\nu - \alpha_2 r - \alpha_1\left(r - \alpha_1 e\right)\right) + \alpha_2\left(\nu - \alpha_2 r\right)\right) + \dot{M}(q)\ddot{q}_d \\ & + M(q)q_d^{(3)} + \dot{C}(q,\dot{q})\dot{q} + C(q,\dot{q})\left(\ddot{q}_d - \nu + \alpha_2 r + \alpha_1 r - \alpha_1^2 e\right) + \dot{G}(q,\dot{q}) + r - \frac{1}{2}\dot{M}(q)\nu \end{aligned} \tag{14}$$

Now consider the following the following auxiliary function

$$N_d(.) = \dot{M}(q_d)\ddot{q}_d + M(q_d)q_d^{(3)} + \dot{C}(q_d,\dot{q}_d)\dot{q} + C(q_d,\dot{q}_d)\ddot{q}_d + \dot{G}(q_d) \tag{15}$$

Adding and subtracting $N_d(.)$ to (14), we obtain

$$M(q)\dot{r} = -\frac{1}{2}\dot{M}(q)r - \dot{\tau}_{RISE}(t) - e_c + \tilde{N}(.) + N_d(.) \tag{16}$$

where $\tilde{N}(.) \triangleq N(.) - N_d(.)$ which can be upper-bounded by an appropriate bound Xian et al. (2004). Using the same reasoning in Xian et al. (2004), the stability of the RISE controller can be easily demonstrated, meaning that $\|e(t)\| \to 0$ as $t \to \infty$, provided that the controller gains α_1, α_2, k_s and β are chosen large enough. The reader is referred to Xian et al. (2004) for the detailed stability proof.

5. Proposed Solution: A RISE-based Adaptive Controller

To enhance the tracking performance of RISE control, it has been reported in Patre et al. (2008) that it can be augmented by a model-based feedforward term. The additional term should compensate for the inherent model nonlinearities and yield improving tracking performance. It should be mentioned however that the dynamics of mechanical manipulators are time-varying and environment-dependant. Moreover, there can be uncertainties in the dynamic parameters such as the masses and inertias. Consequently, it would be relevant to endow the controller with adaptation mechanisms to deal with such issues.

Instead of using RISE term only (12), we propose to control the manipulator with the following augmented control law

$$\tau(t) = \tau_{RISE}(t) + Y_d(.)\ \theta_0, \tag{17}$$

where $Y_d(.) \triangleq Y(q_d, \dot{q}_d, \ddot{q}_d)$, Γ_{RISE} is the RISE control term given by (12) and θ_0 is the nominal vector of parameters formed by best known values of the robot's geometric and dynamic parameters.

In practical situations, the dynamics of the PKM are most likely to vary. A typical example of such a situation is when the PKM is performing pick-and-place of payloads with unknown masses. Consequently, the dynamic parameters of the traveling plate of the PKM will include those of the handled payload. However, the control scheme should automatically identify the dynamic properties of the additional payload in real-time. Consequently, the idea of adaptive control comes directly in mind. Indeed, adaptive strategies are known of their ability to online estimate the dynamics of the system resulting in an enhanced closed-loop performance.

The proposed adaptive controller can be obtained by replacing the nominal parameters vector in (17) by its estimated counterpart $\hat{\theta}(t)$ as follows

$$\tau(t) = \tau_{RISE}(t) + Y_d(.)\ \hat{\theta}(t), \tag{18}$$

where the evolution of estimated parameters vector $\hat{\theta}(t)$ is governed by the following saturation-based adaptation law

$$\dot{\hat{\theta}}(t) = \Gamma\theta_b \,\mathrm{sat}\left(\frac{\Gamma Y_d(.)^T r(t)}{\theta_b}\right), \tag{19}$$

where $\Gamma \in \mathbb{R}^{p\times p}$ is a diagonal adaptation gain matrix with positive elements and θ_b is the maximum allowable bound for the components of the estimated parameter vector θ. The saturation function sat(.) is defined as follows

$$\mathrm{sat}(\xi) = \begin{cases} -1, & \text{for } \xi < 1 \\ \xi, & \text{for } |\xi| \leq 1 \\ 1, & \text{for } \xi > 1 \end{cases} \tag{20}$$

The saturation-based adaptation law (19) ensures that the adaptation parameters remain within allowable range, i.e. $\|\theta\|_\infty \leq \theta_b, \forall t \geq 0$. The adaptation mechanism will adjust the parameters in real-time and feed them to the control law (18) in order to cancel the linear in the parameters dynamics. This adaptation law features some advantageous benefits making it suitable for real-time implementations. First, it has a very simple structure since it is based only on the regression matrix and the combined position-velocity signal. Moreover, it is based on the desired trajectories instead of actual measured ones which might be noisy and inaccurate.

Substituting the proposed control law (18) into the dynamics of the PKM (5) results in the following closed-loop error system:

$$M(q)\nu = Y_d(.)\tilde{\theta}(t) + W(.) - \tau_{RISE}(t), \tag{21}$$

where $\tilde{\theta}(t) \triangleq \theta - \hat{\theta}(t)$ is the parameters' estimation error and the auxiliary function $W(.)$ is given by

$$W(.) = M(q)\left(\ddot{q}_d + \alpha_1\dot{e} + \alpha_2 r\right) + C(q,\dot{q})\dot{q} + G(q) - Y_d(.)\theta. \tag{22}$$

The first time-derivative of (22) is expressed by

$$M(q)\dot{\nu} = -\dot{M}(q)\nu + \dot{Y}_d(.) + Y_d(.)\dot{\hat{\theta}}(t) + \dot{W}(.) - \dot{\tau}_{RISE}(t) \tag{23}$$

After substituting (19) and rearranging the term in (24), the following error dynamics are obtained:

$$M(q)\dot{\nu} = -\frac{1}{2}\dot{M}(q)\nu + \dot{Y}_d(.)\tilde{\theta} + N(.) - \dot{\tau}_{RISE}(t) - r \tag{24}$$

where the auxiliary nonlinear function $N(.)$ is given by:

$$N(.) = -Y_d(.)\dot{\hat{\theta}}(t) + \dot{W}(.) + r - \frac{1}{2}\dot{M}(q)\nu \tag{25}$$

Now, consider another auxiliary nonlinear function $N_d(.)$ obtained by replacing all occurrences of $q, \dot{q}$ and $\ddot{q}$ in (25) by $q_d, \dot{q}_d$ and $\ddot{q}_d$, respectively. Adding and subtracting $N_d(.)$ to the error dynamics (24) yields:

$$M(q)\dot{\nu} = -\frac{1}{2}\dot{M}(q)\nu + \dot{Y}_d(.)\tilde{\theta} - \dot{\tau}_{RISE}(t) - r + \tilde{N}(.) + N_d(.), \tag{26}$$

where $\tilde{N}(.) \triangleq N(.) - N_d(.)$. In a similar manner to Patre et al. (2008), $\tilde{N}(.)$ can be upper-bounded as follows

$$\left\|\tilde{N}(.)\right\| \leq \rho\left(\|z\|\right)\|z\|, \tag{27}$$

where $z(t) \triangleq \left[e^T r^T \nu^T\right]^T$ and $\rho(.)$ is some nondecreasing function.

Based on the definitions of $N_d(.)$ and Y_d, the following upper-bounds can be developed

$$\|N_d(.)\|_\infty \leq \zeta_{N_d}, \qquad \left\|\dot{N}_d(.)\right\|_\infty \leq \zeta_{N_{d2}} \tag{28}$$

$$\|Y_d(.)\|_\infty \leq \zeta_{Y_d}, \qquad \left\|\dot{Y}_d(.)\right\|_\infty \leq \zeta_{Y_{d2}} \tag{29}$$

6. Stability Analysis of the Proposed Controller

Theorem 1: *The joint position and velocity tracking errors ($e(t)$ and $\dot{e}(t)$, respectively) of a PKM whose dynamics is governed by (5) under the controller (18) along with the adaptation law (19) goes to zero as time goes to infinity, provided that the control design parameters α_1 and α_2 are chosen such that $\alpha_1 > 1/2$, $\alpha_2 > 1$, $\beta > \zeta_{N_d} + (\zeta_{N_{d2}}/\alpha_2)$ and that the feedback gain k_s is chosen large enough.*

Proof. ToDo . . . □

7. Real-time Experiments and Results

To demonstrate the relevance of the proposed adaptive RISE-based controller, we implement both original and adaptive RISE controllers on the Delta 3-DOFs robot. Two scenarios are experienced; a nominal case and a robustness to mass variation case.

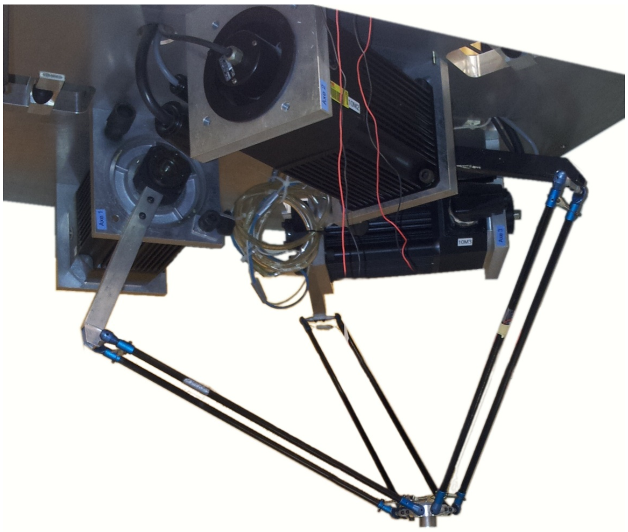

Figure 2. View of the Delta robot used in experiments

Table 2. Parameters of both controllers.

Original RISE		Adaptive RISE	
Parameter	Value	Parameter	Value
α_1	600	α_1	600
k_s	0.43	k_s	0.43
α_2	0.66	α_2	0.66
β	2	β	2
		Γ	0.1

7.1 *Description of the experimental testbed*

The Delta robot is actuated through three direct-drive actuators mounted on the fixed-based providing each one 20 Nm of maximum torque. The motion of the traveling plate is achieved by transmitting the rotations of the actuators to the rear-arms, which themselves are transmitted to the forearms which are linked at the traveling plate through pairs of ball-and-socket passive joints. The particular use of parallel rods for the forearms allows to restrict the motion of the traveling plate to three translations along x, y and z-axes. The development of the control scheme on the EPFL's Delta robot is done with C language via Visual Studio software from Microsoft. The controller is run under a frequency of 1 KHz (sampling time of 1 ms). Figure 2 shows the fabricated 3-DOFs Delta robot which is located in the Robotic Systems Laboratory of EPFL.

The desired trajectories used for this scenario are pick-and-place ones generated according to the method described in Codourey (1998). This method consists of using semi-ellipses for the generation of the desired geometric motion. An illustrative 3D view of the pick-and-place trajectory used in this scenario is shown in Figure 3. Since we are interested in pick-and-place applications, we assume that the mass of the traveling plate is unknown/varying and should be estimated. The nominal values of the remaining dynamic parameters are used since they are not sensitive to payload changes. The parameters of both controllers used in experiments are summarized in Table 2.

7.2 *Performance evaluation criteria*

To evaluate the performance of the proposed controllers, it is necessary to formulate some criteria that allow the quantification of such performance. Since the main objective of the current work is to improve the tracking performance of parallel manipulators, it is then straightforward that the adopted criteria would be based on the tracking errors of the reference trajectories. The solution

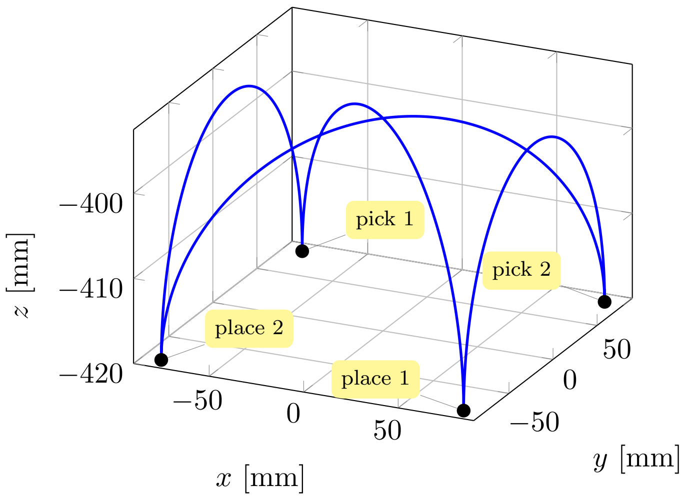

Figure 3. Illustrative view of the experienced pick-and-place trajectory

that is often introduced in the literature is the Root Mean Square Error (RMSE).

Consider the following RMSE criteria based on the computed Cartesian tracking errors

$$RMSE_T = \sqrt{\frac{1}{N}\sum_{k=1}^{N}\left(e_x^2(k) + e_y^2(k) + e_z^2(k)\right)}, \tag{30}$$

where e_x, e_y, e_z denote the position Cartesian tracking error along the x, y and z-axes, respectively, and N is the number of samples.

Similarly, to evaluate the joints tracking performance, we define the following RMSE criteria based on the joint tracking errors

$$RMSE_J = \sqrt{\frac{1}{N}\sum_{k=1}^{N}\left(\sum_{l=1}^{3} e_{q_1}^2(k) + e_{q_2}^2(k) + \cdots + e_{q_l}^2(k)\right)}, \tag{31}$$

where e_{q_i} is the ith joint tracking error.

7.3 *Obtained results*

7.3.1 Scenario 1: nominal case

In this scenario, no additional payload is added to the traveling-plate of the Delta robot. The mass of the traveling-plate is supposed unknown and was initialized to zero ($\hat{m}_p(0) = 0$). The adaptive term has then to estimate the best value of the mass of the traveling-plate in real-time to compensate for its dynamics and yield better tracking accuracy. Notice that the half-masses of the forearms of the robot are also included in $\hat{m}_p$ (due to simplifying hypotheses of the dynamic model).

The Cartesian tracking errors in this scenario for both controllers are depicted in Figure 4. For the sake of clarity, the figures are zoomed in the interval [14,16] seconds. It can be seen that the adaptive RISE controller performs much better than the non-adaptive one. We can also observe the presence of high amplitude spikes in the standard RISE controller that correspond to a stopping of

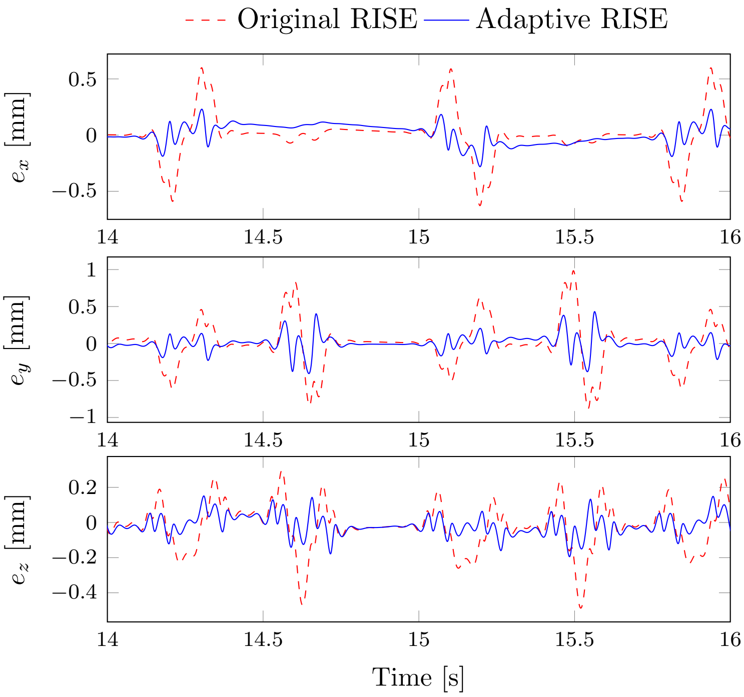

Figure 4. Scenario 1: Cartesian tracking errors.

Table 3. Scenario 1: Summary of the performance of both controllers.

	$RMSE_J$ [deg]	$RMSE_T$ [mm]
Original RISE	0.114	0.454
Adaptive RISE	0.068	0.262
Improvement	40.75 %	42.31 %

the traveling plate at a the end of pick or place trajectory. These spikes are significantly reduced in the adaptive controller.

To quantify the enhancement of the tracking performance brought by the adaptive controller, the previously developed RMSE-based criteria are evaluated for each controller. The obtained results are summarized in Table 3 where it can be seen observed that the tracking improvement of the proposed controller is very significant (up to 42 %).

The generated control input torques for both controllers are shown in Figure 5. For clarity, the plots are zoomed within the interval [14,16] seconds. It can be seen that both signals are in admissible ranges and do not show any high frequency components. It can also be observed that the control effort in the case of the adaptive controller are slightly reduced compared to the non-adaptive one.

Finally, the evolution of the estimated parameter $\hat{m}_p$ versus time is shown in Figure 6. It is worth noting that this parameter corresponds to the mass of the traveling plate in addition to the three half-masses of the forearms.

7.3.2 Scenario 2: robustness to mass variation

In this scenario, an additional payload of 220 g was added to the traveling-plate. Similarly, the estimation loop has to keep updating the unknown parameter $\hat{m}_p$ in real-time until it converges to its real value.

The Cartesian tracking errors for this scenario, which are the most relevant to show, are depicted

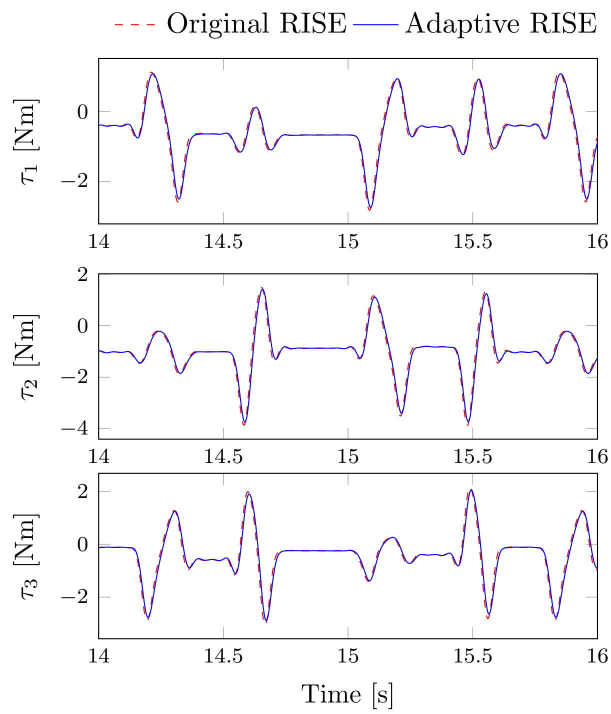

Figure 5. Scenario 1: Evolution of the control inputs.

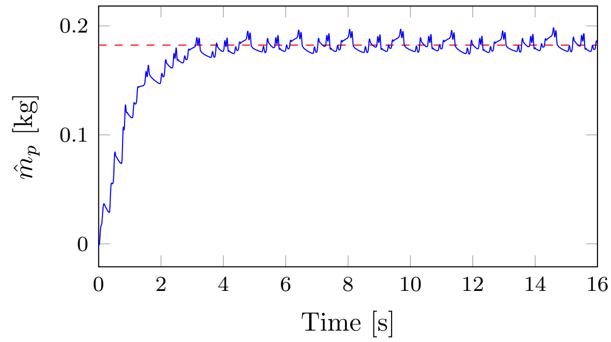

Figure 6. Scenario 1: Evolution of the estimated traveling plate's mass versus time.

Table 4. Scenario 2: Summary of the performance of both controllers.

	$RMSE_J$ [deg]	$RMSE_T$ [mm]
Original RISE	0.182	0.7316
Adaptive RISE	0.0706	0.2746
Improvement	61.21 %	62.47 %

in Figure 7. The plots are focused within the interval [14,16] seconds for clarity. It can be seen that, as expected, the tracking errors are significantly reduced in the case of the adaptive controller compared to the standard non-adaptive one. The improvement can be clearly seen at the occurrences of the spikes which correspond to the end of the current pick or place motion and the starting of the next one.

Table 4 summarizes the tracking performance in terms of the RMS of the errors. It can be noticed that the tracking errors are significantly reduced, even better than in the nominal scenario. Indeed, the tracking errors for this scenario are improved by more than 61 %.

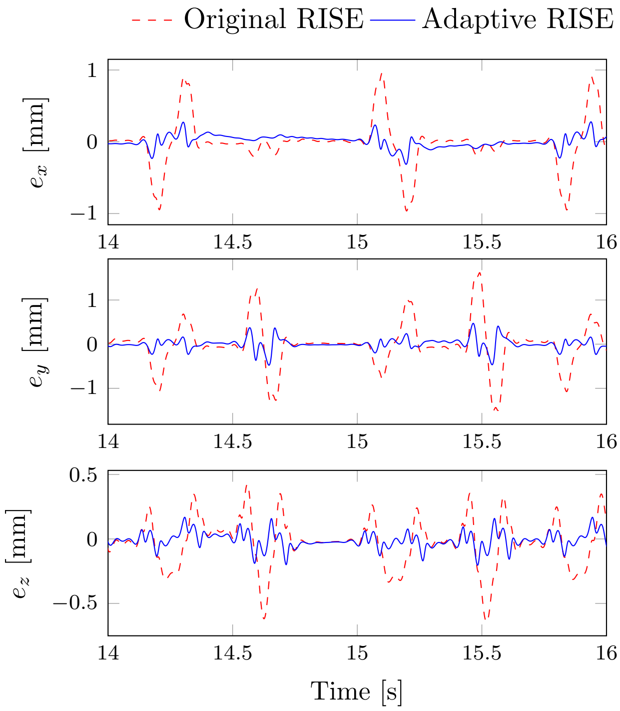

Figure 7. Scenario 2: Cartesian tracking errors.

The evolution of control input torques for both controllers is depicted in Figure 8. For clarity, the plots are zoomed within the time interval [14,16] seconds. Equivalently to the previous scenario, the control efforts are slightly reduced in the adaptive controller.

The evolution of the unknown adaptive parameter $\hat{m}_p$, initialized to zero, is illustrated in Figure 9. Notice that the new estimated value is increased by 220 g compared to the previous scenario, which corresponds to the additional mass added to the traveling-plate.

8. Conclusion

In this paper, an adaptive RISE-based controller for PKMs is proposed. The proposed contribution lies in augmenting the original RISE control law with an adaptive feedforward term to account for the inherent nonlinearities of the system. The proposed solution aims at improving the tracking performance of the closed-loop system by taking advantage of the knowledge about the dynamics in the control-loop. To highlight the benefits of the proposed control strategy, real-time experiments are conducted on a fast 3-DOF Delta robot. Experimental results shows that the proposed RISE-based adaptive controller outperforms original RISE in terms of tracking performance, both in nominal and payload handling scenarios.

References

Asgari, M., & Ardestani, M. (2015). Dynamics and improved computed torque control of a novel medical parallel manipulator: Applied to chest compressions to assist in cardiopulmonary resuscitation. *Journal of Mechanics in Medicine and Biology*, *15*(04).

Bennehar, M., Chemori, A., & Pierrot, F. (2014). A novel rise-based adaptive feedforward controller for redundantly actuated parallel manipulators. In *Ieee/rsj international conference on intelligent robots*

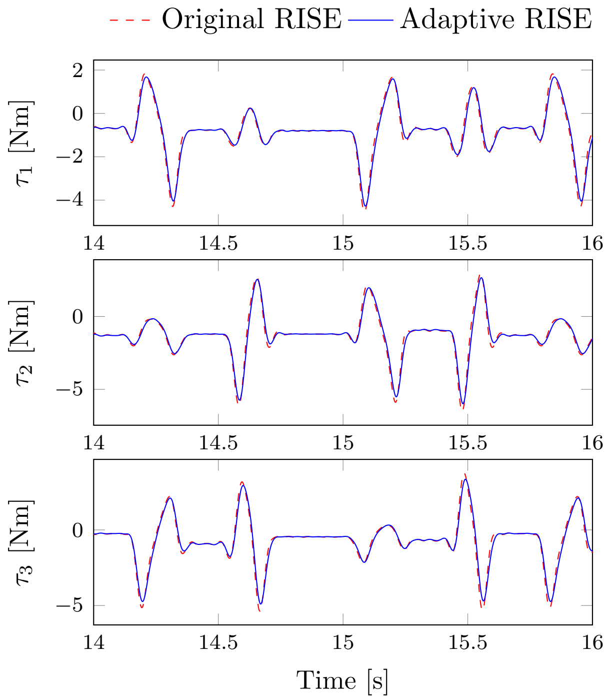

Figure 8. Scenario 2: Evolution of the control inputs.

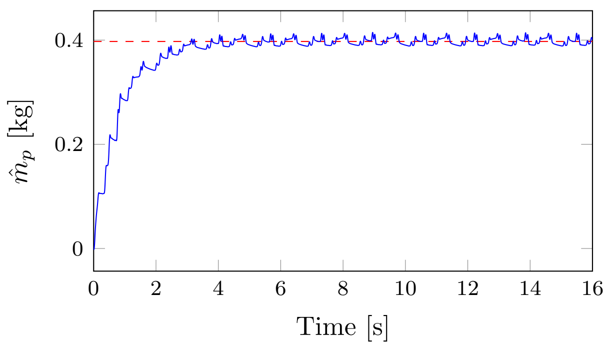

Figure 9. Scenario 2: Evolution of the estimated traveling plate's mass versus time.

and systems (iros'14) (pp. 2389–2394).

Chifu, Y., Qitao, H., Hongzhou, J., O. Ogbobe, P., & Junwei, H. (2010). Pd control with gravity compensation for hydraulic 6-dof parallel manipulator. *Mechanism and Machine Theory*, *45*(4), 666–677.

Clavel, R. (1985, December). *Device for the movement and positioning of an element in space.* Retrieved from `https://patents.google.com/patent/US4976582A` (US Patent 4,976,582)

Codourey, A. (1998). Dynamic modeling of parallel robots for computed-torque control implementation. *The International Journal of Robotics Research*, *17*, 1325–1336.

Company, O., Pierrot, F., Krut, S., Baradat, C., & Nabat, V. (2011). Par2: a spatial mechanism for fast planar two-degree-of-freedom pick-and-place applications. *Meccanica*, *46*(1), 239–248.

Connolly, C. (2007). Abb high-speed picking robots establish themselves in food packaging. *Industrial Robot : An Inter- national Journal*, *34*(4), 281–284.

Craig, J. J., Hsu, P., & Sastry, S. S. (1987). Adaptive control of mechanical manipulators. *The International Journal of Robotics Research*, *6*(2), 16-28.

Dachang, Z., Yanping, F., & Yuefa, F. (2005). A novel parallel manipulator design for packaging and assembly. In *International conference on electronic packaging technology* (pp. 74–78).

Deblaise, D., & Maurine, P. (2005). Effective geometrical calibration of a delta parallel robot used in neurosurgery. In *Ieee/rsj international conference on intelligent robots and systems (iros'05)* (pp. 1313–1318).

Fischer, N., Hughes, D., Walters, P., Schwartz, E., & Dixon, W. (2014). Nonlinear rise-based control of an autonomous underwater vehicle. *IEEE Transactions on Robotics*, *30*(4), 845–852.

Germain, C., Caro, S., Briot, S., & Wenger, P. (2013). Singularity-free design of the translational parallel manipulator irsbot-2. *Mechanism and Machine Theory*, *64*, 262–285.

He, J., Jiang, H., Cong, D., & Ye, J. W., Z. M. an Han. (2007). A survey on control of parallel manipulator. *Key Engineering Materials*, *339*, 307–3013.

Honegger, M., Codourey, A., & Burdet, E. (1997). Adaptive control of the hexaglide, a 6 dof parallel manipulator. In *Robotics and automation, 1997. proceedings., 1997 ieee international conference on* (Vol. 1, pp. 543–548).

Kiam, H. A., Chong, G., & Yun, L. (2005). Pid control system analysis, design, and technology. *IEEE Transactions on Control Systems Technology*, *13*(4), 559–576.

Merlet, J. (2006). *Parallel robots, second edition*. Dordrecht, Netherlands: Springer.

Nabat, V., de la O Rodriguez, M., Company, O., Krut, S., & Pierrot, F. (2005, August). Par4: very high speed parallel robot for pick-and-place. In *Ieee/rsj international conference on intelligent robots and systems (iros'05)* (pp. 553–558).

Ortega, R., & Spong, M. W. (1989). Adaptive motion control of rigid robots: A tutorial. *Automatica*, *25*(6), 877–888.

Patel, Y. D., & George, P. M. (2012). Parallel manipulators applications – a survey. *Modern Mechanical Engineering*, *2*(3), 57–64.

Patre, P., MacKunis, W., Makkar, C., & Dixon, W. (2008). Asymptotic tracking for systems with structured and unstructured uncertainties. *IEEE Transactions on Control Systems Technology*, *16*(2), 373–379.

Sadegh, N., & Horowitz, R. (1990). Stability and robustness analysis of a class of adaptive controllers for robotic manipulators. *The International Journal of Robotics Research*, *9*(3), 74–92.

Sartori Natal, G., Chemori, A., Michelin, M., & Pierrot, F. (2012). A dual-space feedforward pid control of redundantly actuated parallel manipulators with real-time experiments. In *Ifac conference on advances in pid contro (pid'12)*.

Sartori Natal, G., Chemori, A., & Pierrot, F. (2015). Dual-space control of extremely fast parallel manipulators: Payload changes and the 100g experiment. *IEEE Transactions on Control Systems Technology*, *23*(4), 1520-1535.

Sartori Natal, G., Chemori, A., Pierrot, F., & Company, O. (2010). Control of parallel manipulators for very high accelerations : the mechanical vibrations issue. In *11th pan-american congress of applied mechanics (pacam xi)*.

Shang, W., & Cong, S. (2010). Nonlinear adaptive task space control for a 2-dof redundantly actuated parallel manipulator. *Nonlinear Dynamics*, *59*(1-2), 61–72.

Shang, W., Cong, S., & Ge, Y. (2012). Adaptive computed torque control for a parallel manipulator with redundant actuation. *Robotica*, *30*(3), 457–466.

Shayya, S., Krut, S., Company, O., Baradat, C., & Pierrot, F. (2014a). Dimensional synthesis of 4 dofs (3t-1r) actuatedly redundant parallel manipulator based on dual criteria: Dynamics and precision. In *Ieee/rsj international conference on intelligent robots and systems (iros'14)* (pp. 1716–1723).

Shayya, S., Krut, S., Company, O., Baradat, C., & Pierrot, F. (2014b). A novel (3t-2r) parallel mechanism with large operational workspace and rotational capability. In *Ieee international conference on robotics and automation (icra'14)* (pp. 5712–5719).

Siciliano, B., Sciavicco, L., Villani, L., & Oriolo, G. (2009). *Robotics: modelling, planning and control*. London, United Kingdom: Springer Science & Business Media.

Taktak-Meziou, M., Chemori, A., Ghommam, J., & Derbel, N. (2015). Rise feedback with nn feedforward control of a servo-positioning system for track following in hdd. *Transactions on Systems, Signals & Devices*, *10*(1), 1–23.

Xian, B., Dawson, D., de Queiroz, M., & Chen, J. (2004). A continuous asymptotic tracking control strategy for uncertain nonlinear systems. *IEEE Transactions on Automatic Control*, *49*(7), 1206–1211.

Zhang, Y., Cong, S., Shang, W., Li, Z., & Jiang, S. (2007). Modeling, identification and control of a redundant planar 2-dof parallel manipulator. *International Journal of Control Automation and Systems*, *5*(5), 559–569.

Ziegler, J., & Nichols, N. (1942). Optimum settings for automatic controllers. *Transactions of The American*

Society of Mechanical Engineers, *64*(11).